

## NUMERICAL STUDIES OF FLOW THROUGH A WINDBREAK

John D. Wilson  
University of Guelph  
Guelph, Ontario,  
Canada

## 1. Introduction

Numerical solutions to the equations of motion for flow through a porous windbreak have been compared with the experimental data of Bradley and Mulhearn (1983) for flow through a 50% porous slatted fence. The aim of this work is to evaluate closure schemes (turbulence models) and to provide design guidelines for isolated windbreaks and ultimately for multiple windbreaks (windbreak networks). The effect of the windbreak has been parameterised by including in the streamwise-momentum equation a momentum sink of strength  $k_r \bar{u} |\bar{u}| \delta(x,0)$  for a fence/net, or  $c_d a(x,z) \bar{u} |\bar{u}|$  for vegetative shelter (where  $k_r$  is the pressure-loss coefficient of the fence,  $\bar{u}$  is the time average streamwise (x) velocity,  $\delta(x,0)$  is the delta function,  $c_d$  is a drag coefficient,  $a(x,z)$  is the vegetative area density, and  $z$  is the vertical coordinate). A more detailed account of this work is given by Wilson (1985).

## 2. Governing Equations and Closure Schemes

With the x coordinate chosen parallel to the mean flow and the windbreak perpendicular to the flow and of infinite crosswind extent, the mean flow pattern is two-dimensional, and for steady, neutrally-stratified flow the governing equations are

$$\frac{\partial}{\partial x} (\bar{u} \bar{u} + \overline{u'^2} + \frac{\bar{p}}{\rho}) + \frac{\partial}{\partial z} (\bar{u} \bar{w} + \overline{u'w'}) = -k_r \bar{u} |\bar{u}| \delta(x,0) \quad (1a)$$

$$\frac{\partial}{\partial x} (\bar{u} \bar{w} + \overline{u'w'}) + \frac{\partial}{\partial z} (\bar{w} \bar{w} + \overline{w'^2} + \frac{\bar{p}}{\rho}) = 0 \quad (1b)$$

$$\frac{\partial \bar{u}}{\partial x} + \frac{\partial \bar{w}}{\partial z} = 0 \quad (1c)$$

where  $\rho$  is the density,  $\bar{p}$  is the pressure departure from a hydrostatic reference state,  $\bar{w}$  is the mean vertical velocity, and  $\overline{u'^2}$ ,  $\overline{w'^2}$ ,  $\overline{u'w'}$  are components of the Reynold's stress tensor  $\overline{u_i' u_j'}$ .

The numerical solutions discussed herein have been obtained using one or the other of the following closure schemes:

a) Equilibrium Closure, ' $K_0$ -scheme'. The Reynolds stresses are related to mean velocity gradients using eddy viscosity  $K(x,z) = K_0(z) = 0.4 u_{*0} z$  where  $u_{*0}$  is the far upstream friction velocity.

b) ' $k-\epsilon$ '. The eddy viscosity is formed from the turbulent kinetic energy (TKE) and the TKE dissipation rate  $\epsilon$ , for which extra (approximate) transport equations are included (Launder and Spalding, 1974). The ' $k-\epsilon$ ' model was applied to windbreak flow by Hagen et al. (1981) with some success (though in this case the shelter effect entered via the imposition of a measured wind profile at the fence).

c) Launder, Reece, Rodi Second Order Closure, 'LRR20C'. The governing equations are closed using the approximate budget equations for  $\overline{u'^2}$ ,  $\overline{v'^2}$ ,  $\overline{w'^2}$ ,  $\overline{u'w'}$  and  $\epsilon$  described by Launder, Reece, and Rodi (1975) and used by Pope and Whitelaw (1976), who refer to the scheme used here as Reynolds-stress Model II, to predict a number of wake flows. No wall-proximity effect on the pressure strain was included.

## 3. Numerical Method and Boundary Conditions

The flow equations have been solved using the SIMPLE method described by Patankar (1980). The control volume dimensions varied in space to provide highest resolution near the windbreak. The boundary conditions used were:

- a) Upstream: equilibrium neutral surface layer (logarithmic wind profile).  
 b) Downstream:  $\bar{w} = 0$ ,  $\frac{\partial}{\partial x}$  (all other variables) = 0  
 c) Top:  $\bar{w} = 0$ , Reynolds stresses held at far upstream values.  
 d) Ground:  $\bar{w} = 0$ .
- i) ' $k-\epsilon$ '.  $\frac{\partial}{\partial z}$  (TKE) = 0. A local  $u_*$ , formed using a 'wall function' from the lowest  $\bar{u}$ -velocity and the ground-level TKE, determines the dissipation rate at ground and at the first grid-point above ground.

ii) Second order closure. A local  $u_*$ , formed from the lowest velocity  $\bar{u}$ , determines ground-level values of Reynolds stresses and dissipation on the assumption of a shallow local equilibrium layer.

The domain size used was  $[-60 H < x < 112 H, z_0/H < z < 47 H]$  where  $z_0/H$  is the ratio of surface roughness length to windbreak height, and the space was split into 23 (horizontal)  $\times$  24 (vertical) grid volumes. This domain size was chosen after trials to ensure that further removal of boundaries did not affect the solution. Typically solutions (using LRR20C) were obtained within 5 CPU minutes on an IBM 3081 (iterations ceased when a force balance performed around the flow boundaries was correct to within 1%).

#### 4. Results and Discussion

The pressure-loss coefficient of the Bradley and Mulhearn fence (vertical slats of wood,  $1.2 \times 0.08 \times 0.01$  m, 50% porosity) was evaluated in a wind tunnel. A section of the fence was mounted so as to block the tunnel and the ratio  $k_r = \Delta p / \rho u^2$  was measured over the range  $1.5 \text{ ms}^{-1} < u < 6 \text{ ms}^{-1}$ . This yielded  $k_r = 1.97$  (sample standard deviation 0.04) with no discernible speed-dependence, in good agreement with engineering correlation formulae for a sharp edged grid. All simulations used  $k_r = 2.0$  and  $H/z_0 = 600$  (corresponding to the Bradley and Mulhearn experiment) unless otherwise stated.

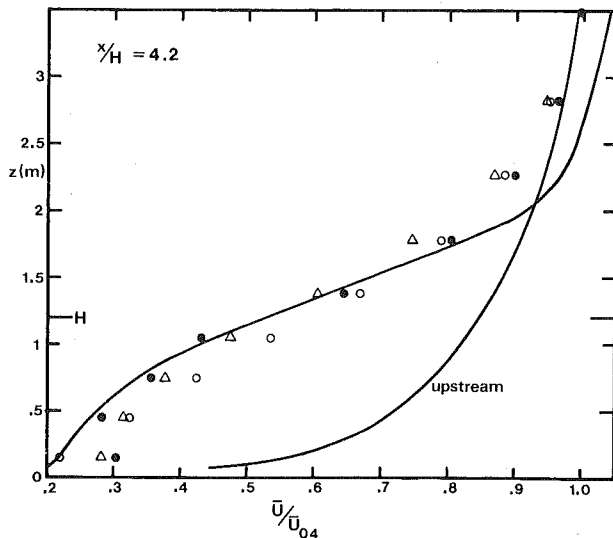


Fig. 1. Vertical profile of horizontal windspeed at  $x/H = 4.2$ . Observations,  $\triangle$ ; LRR20C,  $\bullet$ ;  $k-\epsilon$ ,  $\Delta$ ;  $K_0$ ,  $\circ$ .

Figure 1 compares the observed vertical profile of  $\bar{u}/\bar{u}_{04}$  (where  $\bar{u}_{04}$  is the far upstream speed at  $z = 4$  m) at  $x/H = 4.2$  with the predictions using ' $K_0$ ', ' $k-\epsilon$ ', and 'LRR20C' schemes. The LRR20C prediction is the most satisfactory, giving excellent agreement with observation in the slow-down region. All three predictions share a serious failure to predict correctly the nature of the speed-up over the fence. The predictions conserve the rate of mass flow by generating a weak speed-up over a deep volume rather than, as observed, a marked speed-up over a shallow zone just above the

fence. This poor prediction of the speed-over is presumably responsible for the fact that none of the models gives a satisfactory prediction of the far wake. As can be seen in Fig. 2, a horizontal profile of  $\bar{u}/\bar{u}_{04}$  at fixed heights  $z/H = 0.4, 1.9$ , the predictions give a rate of recovery towards upstream equilibrium which is lower than that observed. It is of interest that the predictions of Pope and Whitelaw (1976) for flow past a disk mounted perpendicular to an approaching airstream show similar features - failure to predict the distinct speed-up in the outer layer (their Fig. 10b) and underprediction of the rate of recovery towards upstream conditions (their Fig. 9a).

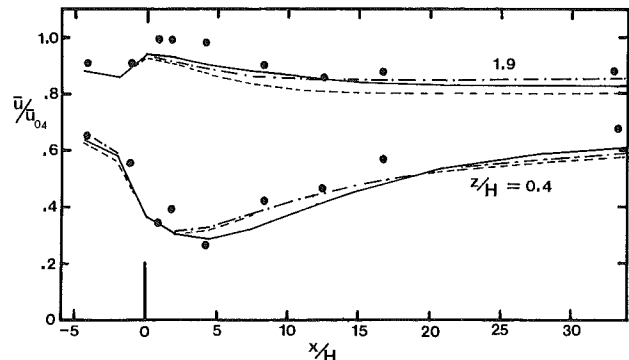


Fig. 2. Horizontal profile of horizontal windspeed at heights  $z/H = 0.4, 1.9$ . Observations,  $\bullet$ ; LRR20C,  $\text{—}$ ;  $k-\epsilon$ ,  $\text{---}$ ;  $K_0$ ,  $\text{-}\cdot\text{-}\cdot\text{-}$ .

Although any of the models examined herein will give a satisfactory estimate of the near-ground maximum velocity deficit (i.e. the peak shelter effect) for an isolated belt, none, at least as presently implemented, could be applied to the problem of multiple windbreaks because of the failure to give the correct rate of recovery. The reason for the good agreement near the windbreak is probably that in this region the pressure gradients are so strong as to dominate the momentum equations, making the stress-gradient parameterisation of secondary importance. Further downstream the pressure gradients are of secondary importance, and stress gradients restore the flow towards equilibrium. Similar findings (best predictions in regions of strongest pressure gradients) have been obtained by others dealing with flows containing sharp pressure gradients.

Mean streamline curvature may have very large effects on shear flow turbulence. Bradshaw (1973) argued that empirical modification of the Reynolds stress and length scale (dissipation) transport equation is necessary to account for curvature effects, which are much larger than would be expected on the basis of the magnitude of the extra terms arising when the equations are re-cast in a coordinate system appropriate to flow curvature. The convex-upwards streamline curvature over the top of the windbreak implies a stabilising (exchange-suppressing) influence which perhaps brings about the shallow distinct speed-up zone observed. The smallest value of the radius of curvature predicted is approximately  $R = 15H$  (at  $x=0, z/H=1$ ). Though there is no obvious choice for shear layer depth  $\delta$ , using  $\delta \sim 10H$  gives  $\delta/R \sim 0.7$ , at which value

strong curvature effects may be expected (Bradshaw, 1969). Incorporation of the curvature correction to the "k-ε" model suggested by Launder et al. (1977), a modification of the ε-destruction term based on a local curvature Richardson number, yielded changes in the numerical solution which did not substantially improve the prediction of the flow over the windbreak. Hanjalic and Launder (1980) described a modification of the ε-equation which they found improved simulation of a boundary-layer with adverse pressure gradient. When included, this modification, which augments the effect of normal strain relative to shear strain on the ε-production term, did not significantly alter the prediction of the LRR20C scheme.

#### 5. A design aid for isolated windbreaks

The 'K<sub>0</sub>' model has been used to generate predictions of the velocity deficit over a range of values of H/z<sub>0</sub> and k<sub>r</sub>. Figure 3 shows an index of "shelter effectiveness"  $S_E = \Delta\bar{u}/\bar{u}_0$  where  $\bar{u}_0$  is the approach speed at  $\frac{z}{H} = 0.4$ , and  $\Delta\bar{u}$  is the velocity deficit relative to approach speed at x/H = 4.4 (approximately the 'most-sheltered' location). A value of  $S_E = 1$  indicates flow reversal. As may be seen, large variations in H/z<sub>0</sub> have little impact, and for given k<sub>r</sub> the shelter effectiveness may be deduced with an expectation of errors not exceeding 20%. Values of k<sub>r</sub> may be related to screen/fence type and porosity with the aid of engineering correlations, such as those given by Hoerner (1965).

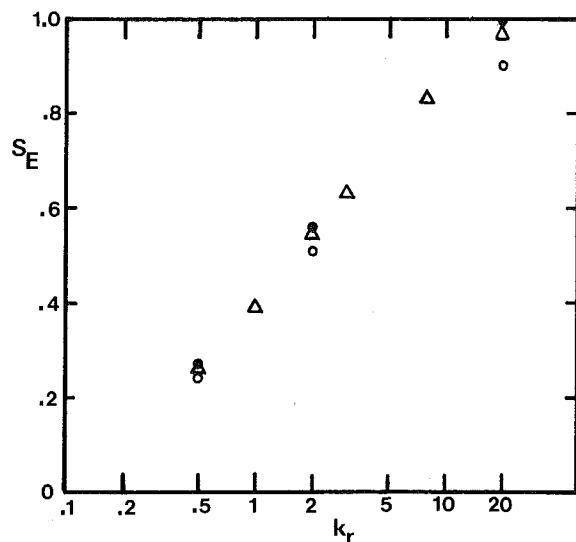


Fig. 3. Shelter effectiveness  $S_E = \Delta\bar{u}/\bar{u}_0$  as a function of pressure-loss coefficient  $k_r$ .  $H/z_0 = 1200$  (●), 600 (Δ), 200 (○).

#### 6. Conclusion

Bradshaw (1973) stated that "the most difficult flows to predict will be those in which a shear layer has its turbulence structure perturbed by a short region of strong pressure gradients and extra rates of strain, and then emerges into a longer region in which its Reynolds stress gradients are significant compared to smaller pressure gradients". The windbreak problem falls into this category, and it is thus not surprising that to date a wholly satisfactory treatment of it (and the general class of flows described above by Bradshaw) has not been found. Nevertheless useful information may be obtained with presently available turbulence models (even, surprisingly, with the crudest of models, the "K<sub>0</sub>"-scheme). For example a fairly accurate prediction of the mean flow pattern near an isolated windbreak has been obtained, permitting the construction of a design graph which relates speed reduction to fence pressure-loss coefficient.

#### 7. References

- Bradley, E.F. and P.J. Mulhearn, 1983: Development of velocity and shear stress distributions in the wake of a porous shelter fence, *J. Wind Eng. and Ind. Aero.*, 15, 145-156.
- Bradshaw, P., 1973: Effects of streamline curvature on turbulent flow, AGARDograph No. 169.
- Bradshaw, P., 1969: The analogy between streamline curvature and buoyancy in turbulent shear flow, *J. Fluid Mech.*, 36, 177-191.
- Hagen, L.J., E.L. Skidmore, P.L. Miller, and J.E. Kipp, 1981: Simulation of effect of wind barriers on airflow, *Trans. ASAE*, 24, 1002-1008.
- Hanjalic, K., and B.E. Launder, 1980: Sensitizing the dissipation equation to irrotational strains, *Trans. ASME J. Fluids Eng.*, 102, 34-40.
- Hoerner, S.F., 1965: *Fluid Dynamic Drag*, published by S.F. Hoerner. Library of Congress Catalog Card Number 64-19666.
- Launder, B.E., C.H. Priddin, and B.I. Sharma, 1977: The calculation of turbulent boundary layers on spinning and curved surfaces, *Trans. ASME J. Fluids Eng.*, 99, 231-239.
- Launder, B.E. and D.B. Spalding, 1974: The numerical computation of turbulent flows, *Computer Methods in Appl. Mechanics and Engineering*, 3, 269-289.
- Patankar, S.V., 1980: *Numerical Heat Transfer and Fluid Flow*, Hemisphere Publishing Co. (Series in Computational Methods in Mechanics and Thermal Sciences).
- Pope, S.B., and J.H. Whitelaw, 1976: The calculation of near-wake flows, *J. Fluid Mech.*, 73, 9-32.
- Wilson, J.D., 1985: Numerical studies of flow through a windbreak, submitted to *J. Wind Eng. and Ind. Aero.*
- Launder, B.E., G.J. Reece, and W. Rodi, 1975: Progress in the development of a Reynolds-stress turbulence closure, *J. Fluid Mech.*, 68, 537-566.